Contribution of the Kv3.1 potassium channel to high-frequency firing in mouse auditory neurones

Lu-Yang Wang, Li Gan, Ian D. Forsythe* and Leonard K. Kaczmarek

*Departments of Pharmacology, Cellular and Molecular Physiology, Yale University School of Medicine, 333 Cedar Street, New Haven, CT 06510, USA and *Ion Channel Group, Department of Cell Physiology and Pharmacology, University of Leicester, PO Box 138, Leicester LE1 9HN, UK*

(Received 25 November 1997; accepted after revision 3 February 1998)

1. Using a combination of patch-clamp, *in situ* hybridization and computer simulation techniques, we have analysed the contribution of potassium channels to the ability of a subset of mouse auditory neurones to fire at high frequencies.

2. Voltage-clamp recordings from the principal neurones of the medial nucleus of the trapezoid body (MNTB) revealed a low-threshold dendrotoxin (DTX)-sensitive current (I_{LT}) and a high-threshold DTX-insensitive current (I_{HT}).

3. I_{HT} displayed rapid activation and deactivation kinetics, and was selectively blocked by a low concentration of tetraethylammonium (TEA; 1 mM).

4. The physiological and pharmacological properties of I_{HT} very closely matched those of the *Shaw* family potassium channel Kv3.1 stably expressed in a CHO cell line.

5. An mRNA probe corresponding to the C-terminus of the Kv3.1 channel strongly labelled MNTB neurones, suggesting that this channel is expressed in these neurones.

6. TEA did not alter the ability of MNTB neurones to follow stimulation up to 200 Hz, but specifically reduced their ability to follow higher frequency impulses.

7. A computer simulation, using a model cell in which an outward current with the kinetics and voltage dependence of the Kv3.1 channel was incorporated, also confirmed that the Kv3.1-like current is essential for cells to respond to a sustained train of high-frequency stimuli.

8. We conclude that in mouse MNTB neurones the Kv3.1 channel contributes to the ability of these cells to lock their firing to high-frequency inputs.

The brainstem binaural auditory pathway computes the localization of a sound source by comparing the relative phase (interaural time differences) and volume (interaural intensity differences) of sound stimuli received at each cochlea. This dual mechanism formed the basis of Lord Raleigh's Duplex Theory for sound localization (Raleigh, 1907). An essential component of this physiological mechanism is the precise preservation of the timing information contained within the auditory signal. For example, neurones of the nucleus magnocellularis and nucleus laminaris lock their firing to the phase of sound frequencies as high as 2 kHz in the chick, and up to 9 kHz in barn owls (Konishi, Takahashi, Wagner, Sullivan & Carr, 1989; Warchol & Dallos, 1990).

In the mammal, globular bushy neurones of the anterior ventral cochlear nucleus (aVCN) and principal neurons in the medial nucleus of the trapezoid body (MNTB) are also capable of firing phase-locked action potentials at over 600 Hz (Guinan, Norris & Guinan, 1972; Brownell, 1975; Wu & Kelly, 1993). The principal neurones of the MNTB are important relay elements that receive a secure synaptic input from the contralateral aVCN via the calyx of Held (Forsythe & Barnes-Davies, 1993) and give an inhibitory projection to the ipsilateral medial and lateral superior olives (MSO and LSO). Both the MSO and LSO also receive direct excitatory projections from the aVCN. The binaural pathway has a number of important adaptations to preserve the fidelity of action potential timing, including two giant excitatory synapses (the endbulb and the calyx of Held), postsynaptic receptors with fast kinetics (Barnes-Davies & Forsythe, 1995; Isaacson & Walmsley, 1995), and low-threshold potassium currents which suppress multiple action potential generation during the decay of synaptic responses (Manis & Marx, 1991; Brew & Forsythe, 1995).

In addition to the above properties, neurones of the MNTB and aVCN have very brief action potentials, which

contribute to enhancing the fidelity and high firing rate of these phase-locking neurones. An important unresolved issue, however, is the mechanism by which the action potential duration is minimized. Previous studies have shown that a *Shaw*-like potassium channel (Kv3.1) is abundantly expressed in neurones that are able to fire at high frequencies, for example cerebellar granule cells (Perney, Marshall, Martin, Hockfield & Kaczmarek, 1992; Weiser *et al.* 1994) and some inhibitory interneurones (Lenz, Perney, Qin, Robbins & Chesselet, 1994; Du, Zhang, Weiser, Rudy & McBain, 1996). Particularly high expression of Kv3.1 mRNA and protein is found in neurones of the rat auditory brainstem (Perney *et al.* 1992; Perney & Kaczmarek, 1997). The Kv3.1 channel has a number of features that help to distinguish it from other potassium channels. For example, it has a high activation threshold (−20 mV), and very rapid activation and deactivation kinetics (Luneau *et al.* 1991; Critz, Wible, Lopez & Brown, 1993; Grissmer *et al.* 1994; Kanemasa, Gan, Perney, Wang & Kaczmarek, 1995; also see review by Chandy & Gutman, 1995). Based on these properties, we have previously constructed a computer model which predicted that such a channel shortens the width of action potentials without truncating their amplitude (Kanemasa *et al.* 1995). We have also suggested that this channel may play a critical role in allowing auditory neurones to follow high-frequency synaptic inputs (Perney & Kaczmarek, 1997).

Brew & Forsythe (1995) have shown that a high-threshold potassium current is present in rat MNTB neurones and have speculated that the properties of this current match those of Kv3.1. There has been, however, no direct quantitative comparison between this current and that of Kv3.1, nor have experiments yet addressed how this current contributes to the ability of these neurones to fire at high frequencies. Because MNTB neurones are specialized to phase lock their action potential firing to high-frequency inputs, we have chosen mouse MNTB neurones as an experimental model system to test our simulation-based predictions (Kanemasa *et al.* 1995; Perney & Kaczmarek, 1997). Since it is not known whether mouse MNTB neurones express this channel, we have conducted *in situ* hybridization experiments to show that the Kv3.1 gene is indeed expressed in these neurones. Furthermore, we demonstrated a strong biophysical and pharmacological correlation between a native high-threshold potassium current in MNTB neurones and Kv3.1 currents expressed in Chinese hamster ovary (CHO) cells. We further investigated the functional role of this potassium current in high-frequency firing by using tetraethylammonium (TEA), a potassium channel blocker known to inhibit the Kv3.1 current at low concentrations (IC_{50}, ~0·2 mM) (Critz *et al.* 1993; Grissmer *et al.* 1994; Kanemasa *et al.* 1995). We have found that blockade of this high-threshold current has little effect on the firing capability of MNTB neurones at frequencies up to 200 Hz. Only at higher frequencies (i.e. 300–400 Hz) do deficits in their firing capability become apparent. This result has also been confirmed by a computer model using various conductances directly obtained from mouse MNTB neurones. Collectively, our results provide compelling evidence that the Kv3.1 channel enables auditory neurones to follow high-frequency stimulation.

METHODS

Preparation of brainstem slices

Slices were prepared as previously described (Barnes-Davies & Forsythe, 1995). Briefly, postnatal mice (129SV/EMS, Jackson Laboratory, Bar Harbor, ME, USA) of age 8–14 days were decapitated and the brains rapidly removed and submerged in an ice-cold bicarbonate-buffered artificial cerebrospinal fluid (ACSF) solution gassed with 95% O_2, 5% CO_2. The solution contained (mM): 125 NaCl, 2·5 KCl, 26 $NaHCO_3$, 1·25 NaH_2PO_4, 2 sodium pyruvate, 3 *myo*-inositol, 10 glucose, 2 $CaCl_2$ and 1 $MgCl_2$ (pH 7·4). The brainstem was glued to a Vibratome stage (Lancer Series 1000, Technical Products International, St Louis, MO, USA) and the area containing MNTB nuclei was cut into four to six transverse slices. The slices were then incubated at 37 °C for 1 h and thereafter kept at room temperature (20–22 °C) for recording.

Stable expression of the Kv3.1 channel in a CHO cell line

Chinese hamster ovary cells with dihydrofolate reductase (DHFR) deficiency (CHO/DHFR(−)) were maintained in Iscove's modified Dulbecco's medium (Gibco) supplemented with 10% fetal bovine serum, 2 mM glutamine, 0·1 mM hypoxanthine and 0·01 mM thymidine in a 5% CO_2 air environment at 37 °C. Cells were seeded 1 day before transfection at about 5×10^5 cells per 60 mm plate. Kv3.1b expression vector (pRC/CMV-Kv3.1, 5 μg) was added 24 h later to transfect CHO/DHFR(−) using lipofectamine (Gibco). The cells were then grown in normal media for 48 h to develop antibiotic resistance and subsequently exposed to geneticin (0·5 mg ml^{-1}, Gibco) for another 10–14 days. The geneticin-resistant cells were subjected to single-cell sorting using FACSIV (Becton Dickenson, San Jose, CA, USA) to generate individual stable cell lines.

Electrophysiological recordings

A slice (or coverslip for CHO–Kv3.1) was transferred to a recording chamber mounted on an Olympus microscope fitted with Nomarski optics and a ×40 water immersion objective. The chamber was continuously perfused (1 ml min^{-1}) with gassed ACSF. Whole-cell recordings were made from visually identified MNTB neurones. An Axopatch-2D amplifier (Axon Instruments) was used for all voltage-clamp recordings. To minimize the distortion of action potential waveform using conventional patch-clamp amplifiers (Magistretti, Mantegazza, Guatteo & Wanke, 1996), an Axoclamp-2A amplifier was also used in bridge-balance mode for some current-clamp recordings (i.e. Fig. 5*A* and *B*). However, we did not present a quantitative analysis of the action potential waveform, because current-clamp recordings using patch-clamp amplifiers (Magistretti *et al.* 1996) may not be adequate to measure accurately the extremely brief action potentials of MNTB neurones. The patch electrodes were pulled from thin-wall borosilicate glass with filament (WPI, Sarasota, FL, USA) using a Narashige P-83 two-stage puller. These electrodes had a resistance of 2–4 MΩ when filled with an intracellular solution containing (mM): 97·5 potassium gluconate, 32·5 KCl, 5 EGTA, 10 Hepes and 1 $MgCl_2$ (pH 7·2), and immersed in ACSF solution. For voltage-clamp recordings from MNTB neurones, the extracellular calcium concentration was lowered to 0·5 mM to minimize the contribution of Ca^{2+}-activated K^+ channels. In addition, TTX (0·5 μM) was also included in ACSF

to block sodium currents in MNTB neurones (typically 5–10 nA at −20 mV). The mean cell capacitance for MNTB neurones and CHO cells was 12·0 ± 0·4 and 13·4 ± 0·3 pF, respectively. The mean series resistance for MNTB neurones and CHO cells was 5·3 ± 0·4 and 4·7 ± 0·7 MΩ, respectively. The compensation for series resistance was set to at least 85% with a lag of 10 μs. Data were filtered at 5 kHz, digitized and acquired on-line with pCLAMP 6 software (Axon Instruments) running on a 486 PC. Analysis of current amplitude and single exponential fitting was performed using the same software. Averaged data are expressed as means ± S.E.M.

In situ hybridization

Digoxigenin-labelled antisense RNA probe was transcribed with T7 polymerase after linearization of the plasmid with *Bam*HI. The resulting probe represents 405 bp of the 3′ end of the mKv3.1 gene and the yield of antisense was quantified using a dot test (Boehringer Mannheim).

The mouse brain was dissected out immediately after decapitation and blocked in OCT solution (Miles Inc., Elkhart, IN, USA) at −30 °C. The tissue was cut into 14 μm thick sections on a 2800 Frigocut cryostat. Sections were thaw-mounted onto silanized glass slides and stored at −70 °C until the time of assay. The tissue sections were postfixed in 4% paraformaldehyde for 1 h, and then put into 1 μg ml^{-1} proteinase K solution for 10 min and treated with 0·25% acetic acid in 0·1 M triethanolamine (pH 8·0) for 10 min. After dehydration in a series of graded alcohols, the sections were prehybridized for 2 h at 55 °C in hybridization buffer (75% deionized formamide, 10% dextran sulphate, 3 × SSC (150 mM NaCl, 15 mM sodium citrate; pH 7·0), 50 mM Na_2HPO_4, 0·02% Ficoll, 0·02% polyvinylpyrrolidone, 0·02% bovine serum albumin, 0·1 mg ml^{-1} denatured salmon sperm DNA and 200 μg ml^{-1} yeast tRNA, pH 7·4). Hybridization of the tissue sections with about 1 ng ml^{-1} riboprobe was carried out at 55 °C for 16–20 h in the same buffer. They were washed three times in 2 × SSC followed by treatment with 200 μg ml^{-1} RNase for 30 min at 37 °C, subsequently washed in 0·5 × and 0·1 × SSC at 55 °C for 1 h each and in TBS buffer (0·1 M Tris-Cl, 150 mM NaCl, pH7·4) three times. Washed sections were blocked in 0·1 M Tris-Cl buffer (pH 7·4) with 5% dry milk for 1 h. They were then incubated with sheep antidigoxigenin Fab fragments conjugated with alkaline phosphatase (Boehringer Mannheim) diluted 1 : 500 in blocking solution for 24 h at 4 °C. The sections were washed three times in TBS for 5 min each and in 10 mM Tris-Cl buffer (pH 9·5) containing 150 mM NaCl and 10 mM $MgCl_2$. The antibody-conjugated alkaline phosphatase was visualized by reaction with 4-nitroblue tetrazolium chloride and 5-bromo-4-chloro-3-indolyl-phosphate (Boehringer Mannheim) in the presence of levamisole (Vector Laboratories, Burlingame, CA, USA) conducted overnight in darkness. The colour reaction was stopped with 10 mM Tris-Cl, 1 mM EDTA (pH 8·0) buffer. The coverslips were mounted with Hydromount (National Diagnostic, Atlanta, GA, USA) for analysis.

Numerical simulations

The responses of MNTB neurones to depolarizing current pulses were simulated using the equation:

$$C(\mathrm{d}V/\mathrm{d}t) = I_{\mathrm{HT}} + I_{\mathrm{LT}} + I_{\mathrm{Na}} + g_{\mathrm{L}}(E_{\mathrm{L}} - V) + I_{\mathrm{ext,t}},$$

where I_{Na} is voltage-dependent sodium current, g_{L} represents a leakage conductance (0·002 μS), E_{L} (−57 mV) and E_{K} (−80 mV) are the reversal potentials for the leakage conductance and potassium conductance, respectively, and C is the cell capacitance (0·01 nF). External currents ($I_{\mathrm{ext,t}}$) were presented as repeated current steps (1·4 nA, 0·25 ms) applied at frequencies from 100 to 400 Hz.

The voltage dependence of I_{HT}, the high-threshold Kv3.1-like current, was modelled using an equation of the form:

$$I_{\mathrm{HT}} = g_{\mathrm{HT}} n^3(1 - \gamma + \gamma p)(E_{\mathrm{K}} - V),$$

where $0 > \gamma > 1$.

The evolution of the variables n and p was described by the differential equations:

$$\mathrm{d}j/\mathrm{d}t = \alpha_{\mathrm{j}}(1 - j) - \beta_{\mathrm{j}}, \quad (1)$$

where $\alpha_{\mathrm{j}} = k_{\alpha\mathrm{j}} \exp(\eta_{\alpha\mathrm{j}} V)$, $\beta_{\mathrm{j}} = k_{\beta\mathrm{j}} \exp(\eta_{\beta\mathrm{j}} V)$ and $j = n, p$.

$k_{\alpha\mathrm{j}}$, $k_{\beta\mathrm{j}}$, $\eta_{\alpha\mathrm{j}}$ and $\eta_{\beta\mathrm{j}}$ are constants that determine the rates and voltage dependence of current activation. The sodium current I_{Na} and the low threshold potassium current I_{LT} were simulated by the equations:

$$I_{\mathrm{LT}} = g_{\mathrm{LT}} l r(E_{\mathrm{K}} - V),$$

$$I_{\mathrm{Na}} = g_{\mathrm{Na}} m^3 h(50 - V),$$

with the evolution of the variables l, r, m and h given by eqn (1), with $j = l, r, m, h$, and where g_{LT} and g_{Na} represent the conductance for the low threshold potassium current and the sodium current, respectively.

The parameters for the voltage dependence and kinetics of I_{HT} were slightly modified from those of Kanemasa *et al.* (1995) and those of Perney & Kaczmarek (1997) for Kv3.1 currents in NIH-3T3 cells and were obtained from direct fits to traces recorded from MNTB neurones and CHO cells at several different potentials: $g_{\mathrm{HT}} = 0{\cdot}15$ μS (Fig. 5*C*) or $g_{\mathrm{HT}} = 0$ (Fig. 5*D*), $\gamma = 0{\cdot}1$, $k_{\alpha\mathrm{n}} = 0{\cdot}2719$ ms^{-1}, $\eta_{\alpha\mathrm{n}} = 0{\cdot}04$ mV^{-1}, $k_{\beta\mathrm{n}} = 0{\cdot}1974$ ms^{-1}, $\eta_{\beta\mathrm{n}} = 0$ mV^{-1}, $k_{\alpha\mathrm{p}} = 0{\cdot}00713$ ms^{-1}, $\eta_{\alpha\mathrm{p}} = -0{\cdot}1942$ mV^{-1}, $k_{\beta\mathrm{p}} = 0{\cdot}0935$ ms^{-1} and $\eta_{\beta\mathrm{p}} = 0{\cdot}0058$ mV^{-1}). Parameters for I_{LT} were also obtained by a direct fit to traces recorded from mouse MNTB neurones and these were: $g_{\mathrm{LT}} = 0{\cdot}02$ μS, $k_{\alpha\mathrm{l}} = 1{\cdot}2$ ms^{-1}, $\eta_{\alpha\mathrm{l}} = 0{\cdot}03512$ mV^{-1}, $k_{\beta\mathrm{l}} = 0{\cdot}2248$ ms^{-1}, $\eta_{\beta\mathrm{l}} = -0{\cdot}0319$ mV^{-1}, $k_{\alpha\mathrm{r}} = 0{\cdot}0438$ ms$^{-1,}$ $\eta_{\alpha\mathrm{r}} = -0{\cdot}0053$ mV^{-1}, $k_{\beta\mathrm{r}} = 0{\cdot}0562$ ms^{-1} and $\eta_{\beta\mathrm{r}} = -0{\cdot}0047$ mV^{-1}. Corresponding parameters for the sodium current were: $g_{\mathrm{Na}} = 0{\cdot}5$ μS, $k_{\alpha\mathrm{m}} = 76{\cdot}4$ ms$^{-1,}$ $\eta_{\alpha\mathrm{m}} = 0{\cdot}037$ mV^{-1}, $k_{\beta\mathrm{m}} = 0{\cdot}0381$ ms^{-1}, $\eta_{\beta\mathrm{m}} = -0{\cdot}043$ mV^{-1}, $k_{\alpha\mathrm{h}} = 0{\cdot}00013$ ms$^{-1,}$ $\eta_{\alpha\mathrm{h}} = -0{\cdot}1216$ mV^{-1}, $k_{\beta\mathrm{h}} = 1{\cdot}999$ ms^{-1} and $\eta_{\beta\mathrm{h}} = 0{\cdot}0384$ mV^{-1}.

RESULTS

Current-clamp recordings

We first characterized the firing properties of mouse MNTB neurones using current-clamp recording in the whole-cell patch configuration. The resting potential of these neurones was about −60 mV (59·7 ± 3·1 mV, $n = 19$). Figure 1*A* illustrates the typical change in membrane potential of an MNTB neurone in response to a series of hyperpolarizing and depolarizing current steps. With subthreshold positive current steps, the membrane potential displayed an initial small hump which decayed back to a steady state for the remainder of the current step. Suprathreshold current injection (> 0·1 nA) usually evoked one to three action potentials at the beginning of the current step, with no further spike generation thereafter. The first action potential always occurred within the initial 5 ms of current injection with little variability in latency, suggesting that this may be an important property by which these neurones preserve the timing of an input signal. Figure 1*D* summarizes these changes in the membrane potential

(measured near the end of the current step, $n = 11$). The voltage–current relationship is non-linear and displays strong outward rectification above the resting potential of −60 mV, indicating that outward conductances are likely to determine the firing pattern of MNTB neurones.

Voltage-gated potassium currents regulate both action potential repolarization and firing rates on depolarization. We examined the effects of two potassium channel blockers, TEA and dendrotoxin (DTX). DTX (100 nM) had little effect on the height or width of individual action potentials evoked by a short pulse (0·5 ms, 1·5 nA; data not shown) but produced a striking enhancement in the number of action potentials generated in response to a sustained depolarizing current injection (Fig. 1*B*). This could also be seen with levels of stimulating current that were sub-threshold under the control condition (Fig. 1*A*), suggesting that DTX blocks a potassium conductance that is active near the resting potential. The functional role of this conductance is presumably to reset membrane potential rapidly and prevent repetitive firing following the initial action potential. Addition of a low concentration of TEA (1 mM) in the presence of DTX reduced action potential firing frequency, broadened individual action potentials and induced a progressive decrease in their amplitude during a pulse (Fig. 1*C*). This observation suggests that mouse MNTB neurones possess a TEA-sensitive potassium conductance that enables these cells to fire repetitively at high rates.

Voltage-clamp recordings

To define further the underlying voltage-dependent potassium conductances, whole-cell voltage-clamp recordings were made from MNTB neurones with a low-calcium (0·5 mM) artificial cerebrospinal fluid (ACSF) containing 0·5 μM tetrodotoxin (TTX). Under these conditions, the maximum potassium current (over a voltage range from −80 to +60 mV) was typically more than 15 nA and largely non-inactivating over several hundred milliseconds (Fig. 2*A*, left panel). Activation of voltage-dependent currents could be detected above −60 mV. Addition of TEA (1 mM) produced a pronounced inhibition of the current (to 36·1 ± 6·3 % of the total outward current at +60 mV, $n = 9$), particularly at voltages above −20 mV (Fig. 2*A*, right panel). The current trace at −40 mV (the first trace above baseline) was virtually identical before and after TEA

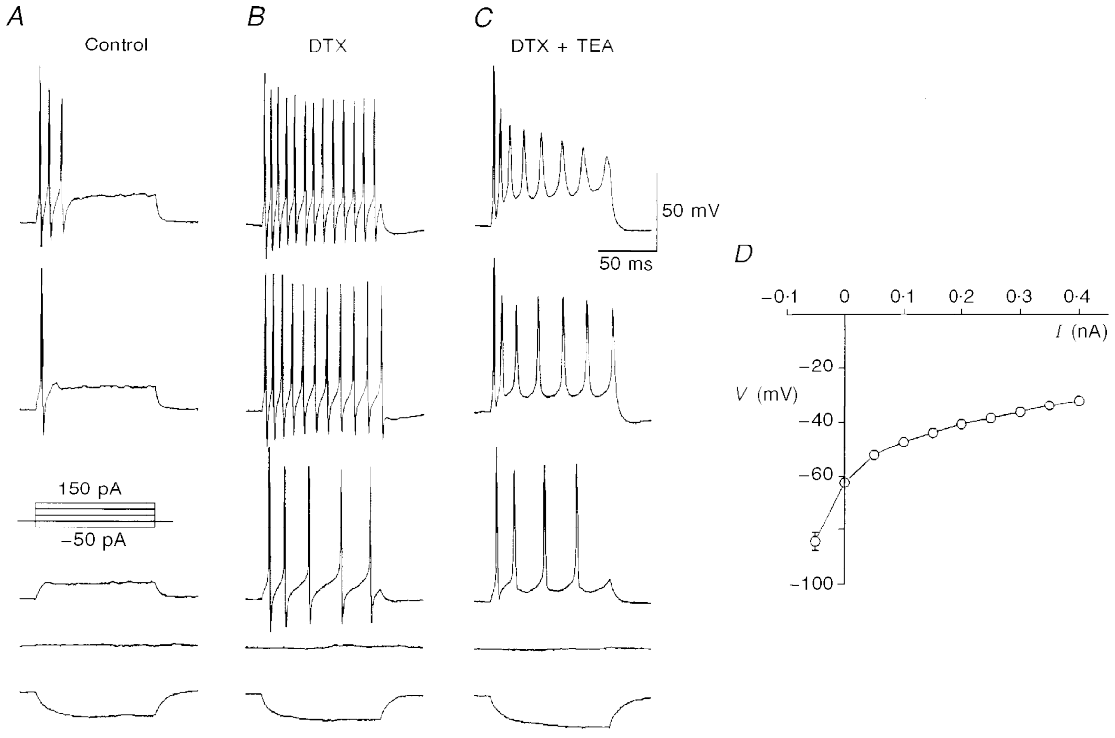

Figure 1. Multiple outwardly rectifying conductances underlying the firing pattern in MNTB neurones

A, the response of a MNTB neurone to a series of current injections from −50 to 150 pA with increments of 50 pA. The resting potential before current injections was about −60 mV. *B*, when this cell was exposed to 100 nM DTX, the number of spikes elicited increased during depolarizing current injections, even at a previously subthreshold current level (50 pA, 3rd trace of the panel). Similar observations were made in three other cells. *C*, co-application of TEA (1 mM) and DTX (100 nM) caused a reduction in both the number and amplitude of spikes in response to the same depolarizing current injections as in *B*. *D*, voltage–current relationship for data averaged from 11 MNTB neurones. The measurement of voltage at different current injection levels was made at 145 ms into the pulse.

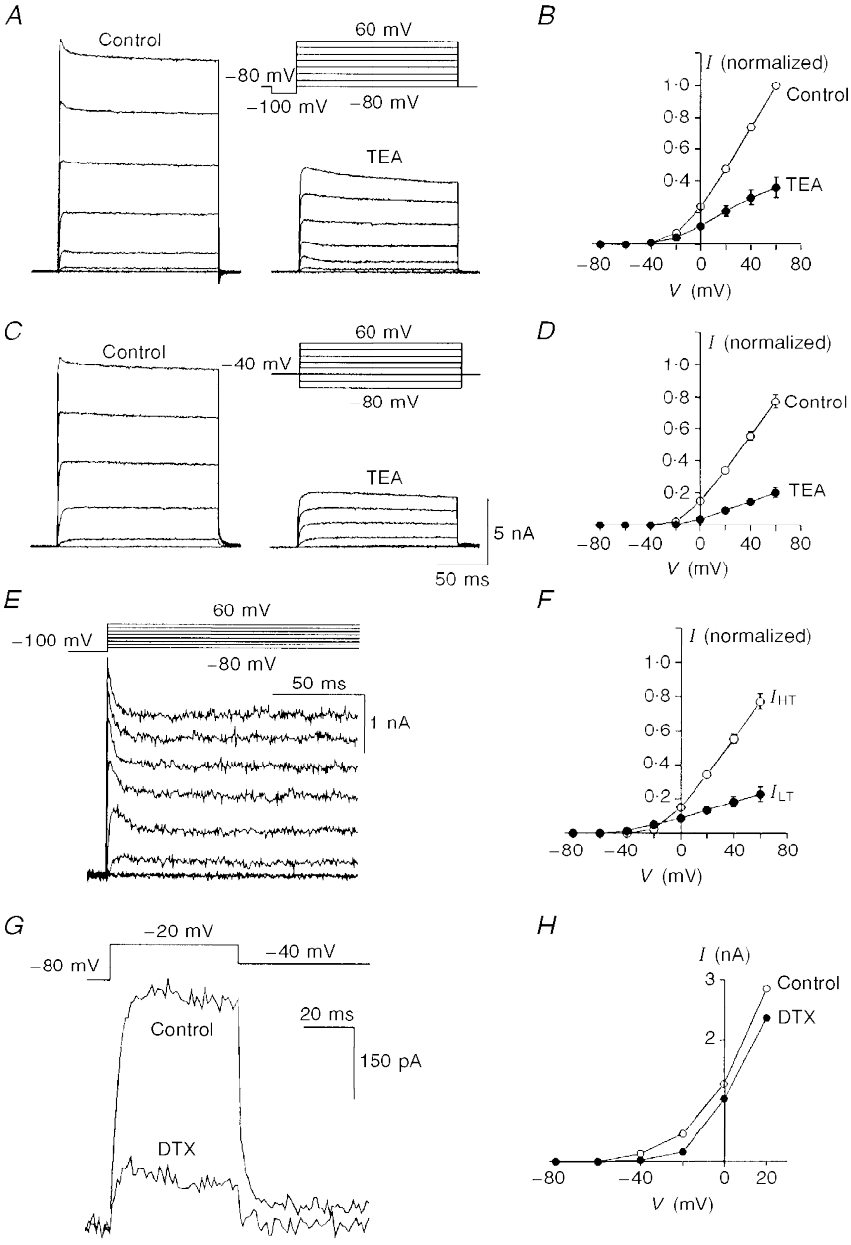

Figure 2. Different components of the voltage-dependent potassium current and their sensitivity to potassium channel blockers

A, the total outward current (left panel) from an MNTB neurone was recorded by stepping from a holding potential of −80 mV to +60 mV in 20 mV increments. Each 200 ms step was preceded by a 30 ms prepulse to −100 mV. Addition of 1 mM TEA blocked a large portion of the current (right panel). *B*, the averaged current–voltage relationship in the absence and presence of TEA. *C*, I_{HT} recorded using the same voltage protocol as in *A* after maintaining the holding potential at −40 mV for 2 min (left panel). The amount of block by TEA (right panel) was increased substantially compared with *A*. *D*, the average current–voltage relationship before and after addition of TEA from a holding potential of −40 mV. *E*, I_{LT} obtained by subtracting I_{HT} in *C* (left panel) from total outward currents in *A* (left panel). *F*, the relative distribution of I_{LT} *versus* I_{HT} is shown in two sets of averaged current–voltage curves. Note that the threshold for activation of I_{LT} is 20 mV more negative than that for I_{HT}. *G*, I_{LT} was recorded directly by stepping from a holding potential of −80 mV to −20 mV. Application of DTX (100 nM) reduced the current to 25·0 ± 2·1 % ($n = 3$) of the control amplitude. *H*, current–voltage relationship from one recording before and after DTX addition. Holding potential was −80 mV. The averaged data plotted in *B*, *D* and *F* ($n = 9$) was taken from measurements made at 195 ms into the pulse. The current amplitude at any given voltage in different cells was normalized to that recorded at +60 mV under control conditions.

application, suggesting that this blocker preferentially inhibited a high-threshold component of the potassium current, with little effect on a low-threshold component. This low-threshold current, however, could be directly inactivated by changing the holding potential from −80 mV to more depolarized potentials (data not shown). Under the condition that the neurone was held at −40 mV for at least 2 min, the high-voltage threshold current (I_{HT}) remained and was blocked by 70–80% by 1 mM TEA (Fig. 2*C*). The normalized current–voltage curves with a holding potential of −40 mV are shown in Fig. 2*B* and *D*. I_{HT} accounted for 77·2 ± 4·3% of the total outward current at a potential of +60 mV and was reduced to 20·2 ± 3·2% of control current by 1 mM TEA ($n = 9$; Fig. 2*D*).

The low-threshold component of outward current (I_{LT}) (Fig. 2*E*) was obtained by subtracting the high-threshold current (in Fig. 2*C*, left panel) from total outward current (in Fig. 2*A*, left panel). This current represented 22·9 ± 4·4% of the total current ($n = 9$) and exhibited partial inactivation shortly after the voltage step (Fig. 2*E*). Figure 2*F* shows the averaged data from these nine MNTB neurones to illustrate the relative amounts of I_{HT} and I_{LT} and their voltage dependence. To resolve I_{LT} further in the absence of I_{HT}, the potential was stepped from −80 to −20 mV (Fig. 2*G*); this current was largely blocked by 100 nM DTX (to 25·0 ± 2·1% of control, $n = 3$). This observation, combined with the current-clamp data, suggests that I_{LT} activates rapidly with relatively small depolarizations and is capable of shunting action potential generation in the MNTB neurone. Comparison of current–voltage relationships before and after addition of DTX clearly showed that the DTX-sensitive and DTX-insensitive currents have a different voltage dependence (Fig. 2*H*), and indicate that I_{HT} was not affected by this toxin.

In situ hybridization

The biophysical features of I_{HT}, such as a high activation threshold (−20 mV) and sensitivity to low concentrations of TEA (1 mM), resemble those of a non-inactivating delayed rectifier (Kv3.1) in the *Shaw* family of potassium channels (Luneau *et al.* 1991; Critz *et al.* 1993; Kanemasa *et al.* 1995). To investigate if the Kv3.1 gene is expressed in mouse MNTB neurones, we conducted *in situ* hybridization experiments using an antisense RNA probe that specifically recognizes the C-terminus of the Kv3.1 gene. Indeed, along the auditory pathway this probe produced strong labelling in MNTB neurones (Fig. 3*A*), and moderate labelling in the dorsal cochlear nucleus (DCN) and ventral posterior cochlear nucleus (VCP). In the cerebellum, granule cells (GR) and Purkinje neurones, but not neurones of the molecular layer, were well labelled (Fig. 3*B*).

Biophysical correlation of the Kv3.1 channel with I_{HT}

To investigate the relationship of Kv3.1 to I_{HT}, we established a stable CHO cell line expressing the Kv3.1 channel. The size of CHO cells (10–15 μm) is similar to that of MNTB neurones and the expression level of the channel (generating about 15 nA at +60 mV) is also comparable to that found in MNTB neurones. Under identical recording conditions, we compared the activation and deactivation kinetics of currents in these cells as well as their sensitivity to TEA. Figure 4*A* and *B* shows two typical recordings made from a MNTB neurone and a CHO cell expressing Kv3.1 (CHO–Kv3.1). The 10–90% rise times for maximal activation ranged from 5·53 ± 0·65 ms at 0 mV to 0·50 ± 0·02 ms at +60 mV in MNTB neurones ($n = 9$) while in CHO–Kv3.1 cells ($n = 6$) the rise times at the corresponding voltages were from 4·36 ± 0·39 to 0·53 ± 0·05 ms, respectively (Fig. 4*C*). The correlation coefficient between these two data sets was 0·998. To determine the deactivation kinetics of I_{HT} and the Kv3.1 current, we compared the tail currents recorded at −20 mV from MNTB neurones and CHO–Kv3.1 cells (Fig. 4*D* and *E*). These currents were well described by a single exponential with comparable time constants of 5·2 ± 0·3 ($n = 9$) and 6·8 ± 0·3 ($n = 6$), respectively (Fig. 4*F*). Perfusion of TEA (1 mM) produced a rapid and profound inhibition of currents from both cell types (75·0 ± 5·9% for nine MNTB neurones, 76·8 ± 2·4% for six CHO–Kv3.1 cells, Fig. 4*G*). The current–voltage relationship for CHO–Kv3.1 cells in the absence and presence of TEA (Fig. 4*H–J*) closely resembled that for MNTB neurones (Fig. 2*D*). Taken together, these observations strongly suggest that in mouse MNTB neurones I_{HT} represents a channel that is composed, in whole or in part, of Kv3.1 protein.

Function of the Kv3.1 channel in MNTB neurones

The rapid activation and deactivation kinetics of the Kv3.1 channel are likely to contribute to the capability of neurones to follow high-frequency synaptic inputs. To test the role of the Kv3.1-like I_{HT} in the ability of MNTB neurones to follow high frequencies, we stimulated MNTB neurones with a train of short stimuli (0·3 ms, 1·5–2 nA) at different frequencies. Full action potentials were observed in all MNTB neurones ($n = 15$) at 300 Hz and in some cases up to 400 Hz (3/15). Figure 5*A* illustrates that one neurone at 400 Hz was able to fire in groups of consecutive action potentials separated by one or two failures. When I_{HT} was blocked by application of TEA (1 mM) (Fig. 5*B*), we found that the cell could still follow stimulation at 100 Hz, even though the action potentials were broadened. At 200 Hz, use-dependent reduction in the amplitude of the action potentials was increased. At 300 Hz, the repolarization between action potentials was severely hampered. Except for the first spike in each train, the cell failed to fire full size action potentials altogether at 400 Hz. These results indicate that the Kv3.1 channel is likely to be essential for MNTB neurones to achieve phase locking at high frequencies.

To examine the function of the Kv3.1-like I_{HT} further, we constructed a computer model to simulate the responses of MNTB neurones to current pulses applied at frequencies up to 400 Hz. For these simulations we used a model similar to that used previously to study the properties of Kv3.1

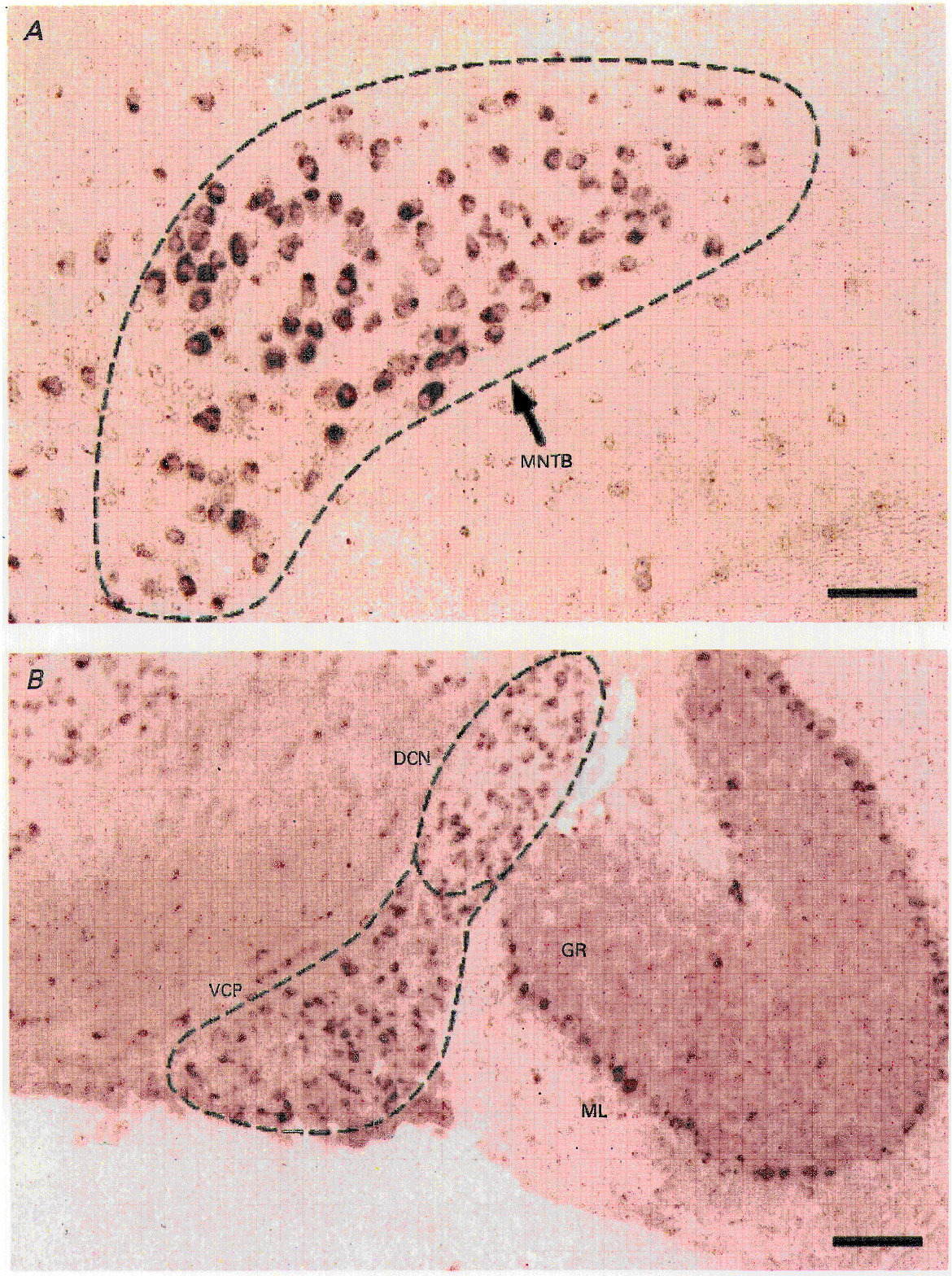

Figure 3. Positive labelling of MNTB neurones by a Kv3.1 antisense probe

A, strong labelling of the principal neurones of the MNTB region. *B*, labelling of neurones in the dorsal cochlear nucleus (DCN), ventral posterior cochlear nucleus (VCP), cerebellar granule cells (GR) and Purkinje neurones. The latter are situated between the molecular layer (ML) and the GR layer. This experiment was performed on a 12-day postnatal mouse. Scale bar, 100 μm.

currents (Kanemasa *et al.* 1995; Perney & Kaczmarek, 1997), but in which the parameters had been altered to match the conductance levels and kinetic properties of I_{HT} and I_{LT} measured directly in the mouse MNTB neurones. The model comprises a single compartment, representing the soma, with a leak conductance, a voltage-dependent sodium current, and potassium currents with the properties of I_{LT} and I_{HT}. The amplitudes of the potassium currents, as well as their voltage dependence and kinetics of activation and inactivation were chosen to match those in the MNTB neurones. Action potentials were triggered by brief (0·25 ms) current pulses with amplitudes (0·8–1·8 nA) similar to those used to stimulate the MNTB neurones. We found that the model could follow current pulses up to about 300 Hz with full action potentials (Fig. 5*C*). When the stimulation frequency was further increased, some of the current pulses failed to trigger action potentials, such that, as in the real neurones, stimulation at 400 Hz resulted in failures between evoked action potentials.

To mimic the block of Kv3.1 by TEA, the Kv3.1-like I_{HT} was eliminated from the model with no change in other parameters. Under these conditions, action potentials followed stimulation at frequencies up to 200 Hz, but significant use-dependent reduction in amplitude occurred at higher frequencies (Fig. 5*D*). At frequencies above 300 Hz full action potentials were triggered only in response to the first stimulus pulse in a train, as also occurs in the real cells. Thus, this simple model indicates that a reduction in the Kv3.1-like current can qualitatively account for the loss of response to high-frequency stimulation.

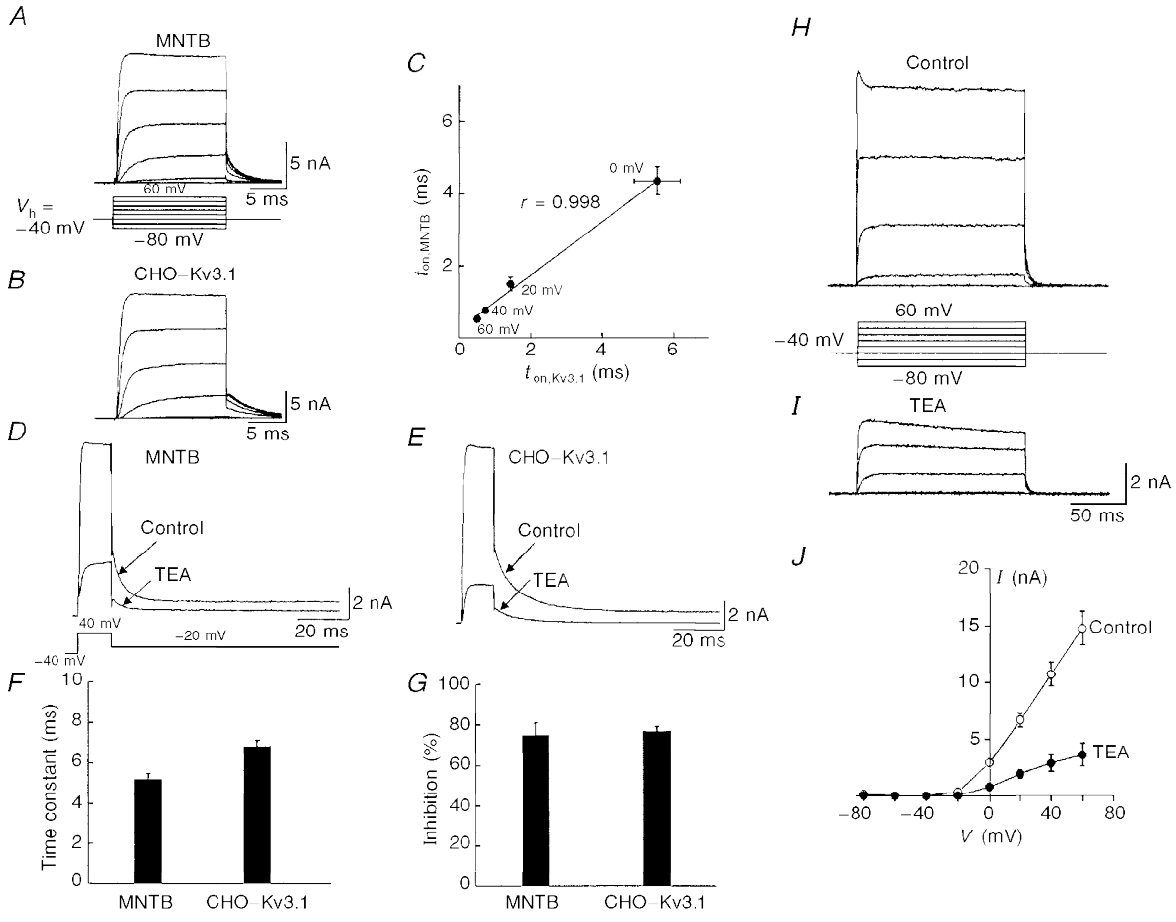

Figure 4. Physiological correlation between I_{HT} and the Kv3.1 current

A and *B*, representative current traces recorded from an MNTB neurone and a CHO–Kv3.1 cell in response to a series of voltage steps from −80 to +60 mV in 20 mV increments. *C*, the 10–90% rise time for maximal activation for MNTB neurones ($t_{on,MNTB}$, $n = 9$) is plotted against that for CHO–Kv3.1 cells ($t_{on,Kv3.1}$, $n = 6$) at different test voltages. *D* and *E*, similar kinetics of the tail currents recorded from an MNTB neurone and a CHO–Kv3.1 cell, and similar block by 1 mM TEA. These tail currents were well fitted by a single exponential function. *F* and *G*, a summary of the time constants calculated from the fitting of tail currents and the extent of block by TEA. *H* and *I*, current traces recorded from a CHO–Kv3.1 cell before and after addition of TEA (1 mM). *J*, the averaged current–voltage curves from seven CHO–Kv3.1 cells. The holding potential for these recordings was −40 mV.

DISCUSSION

We have shown that the TEA-sensitive I_{HT} in mouse MNTB neurones is likely to be a product of the *Shaw* subfamily Kv3.1 channel on the basis of following observations. First, an antisense probe that specifically recognizes Kv3.1 mRNA strongly labelled MNTB neurones. Second, the activation and deactivation kinetics of I_{HT} in MNTB neurones correlated very closely with those of Kv3.1 current expressed in CHO cells. Third, we found that the sensitivity of I_{HT} and the Kv3.1 current to TEA is virtually identical. Moreover, we have shown that block of the I_{HT} conductance in MNTB neurones specifically impairs the ability of these cells to respond to high-frequency stimulation but leaves the response to lower frequencies (< 200 Hz) unimpaired. This experimental result can be mimicked in a numerical simulation of MNTB neurones by elimination of a Kv3.1-like conductance.

While I_{HT} forms the major outward conductance at positive potentials in MNTB neurones, another potassium current, the low-threshold I_{LT}, predominates at membrane potentials near the action potential threshold. These two conductances serve quite different, but complementary, functions in the binaural auditory pathway: I_{HT} minimizes action potential duration, and as we have shown, allows the neurone to follow repetitive inputs at the highest possible frequency. I_{LT} appears to contribute very little to the shape or amplitude of individual action potentials but instead prevents cells from firing multiple spikes in response to prolonged depolarization. Thus, I_{LT} maintains fidelity of transmission so that the output of the MNTB faithfully follows its input via the calyx of Held. Our findings on I_{LT} are consistent with previous studies that have examined characteristics of similar currents in rat MNTB neurones (Brew & Forsythe, 1995) and in neurones of the cochlear nucleus in other

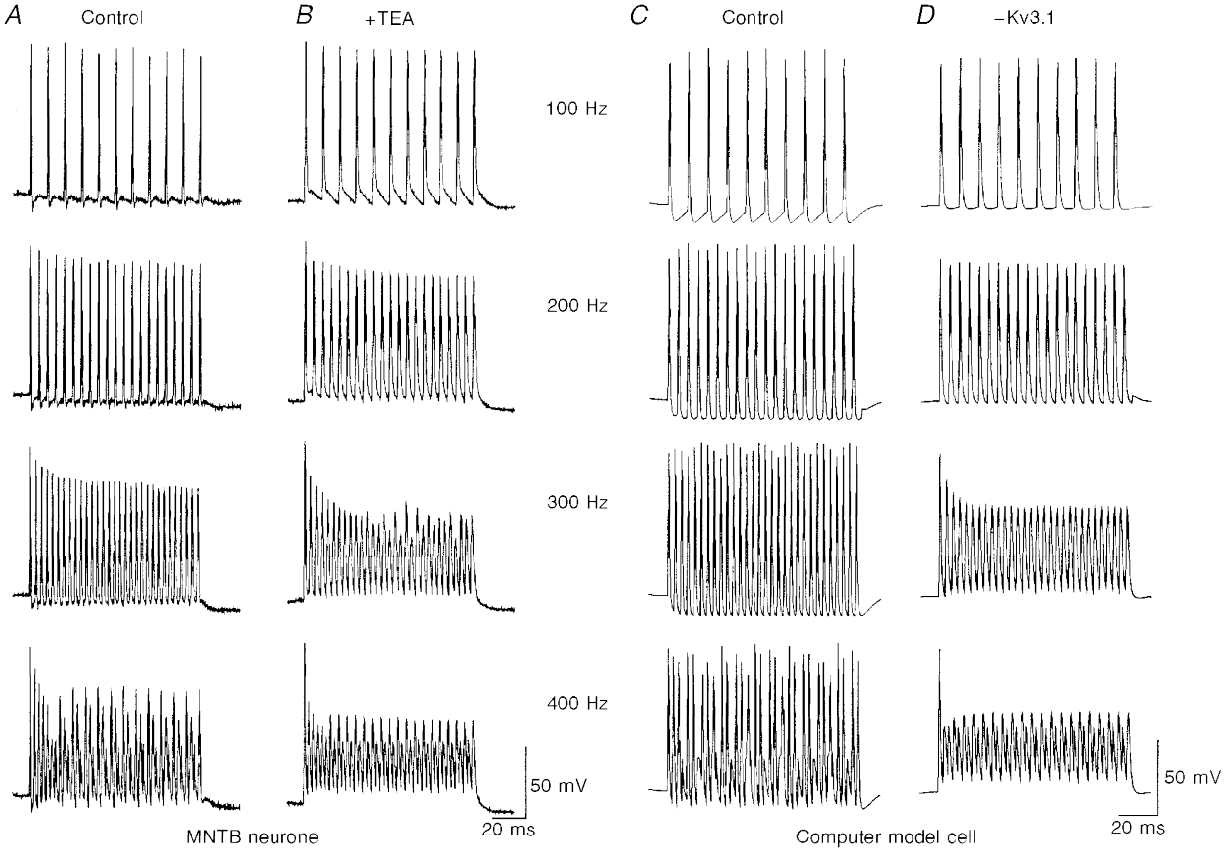

Figure 5. Contribution of I_{HT} to the ability of MNTB neurones or computer-generated model cells to respond to high-frequency stimulation

A, a typical recording from an MNTB neurone showing that a train of action potentials can be evoked by directly injecting short current pulses (2 nA, 0·3 ms) at four different test frequencies (100 to 400 Hz). Some failure in action potential generation can be seen at 400 Hz. *B*, after application of 1 mM TEA, individual action potentials were broadened. At 300 Hz, this neurone failed to fire full-size action potentials after the first 3 or 4 impulses. At 400 Hz, the cell no longer fired normal action potentials (except the first spike of the train) and instead showed slow waves of oscillation. *C*, simulations of a model cell characterized by sodium, I_{LT}- and I_{HT}-like conductances, as well as a leakage conductance. The cell was stimulated by brief current pulses (1·4 nA, 0·25 ms) applied at frequencies from 100 to 400 Hz. *D*, responses of the model cells to the same stimuli after elimination of the I_{HT} conductance.

species (Manis & Marx, 1991; Reyes, Rubel & Spain, 1994; Zhang & Trussell, 1994).

There are some differences between our findings on mouse MNTB neurones and those previously reported for the rat (Brew & Forsythe 1995). In particular, in contrast to the single spike firing pattern that is the typical response of rat MNTB neurones to a depolarization, mouse MNTB neurones tend to fire several spikes near the beginning of a sustained depolarizing current injection. This may be attributed to the lower expression level of I_{LT} in mouse than in rat MNTB neurones. In our experiments, the amplitude of I_{LT} was typically less than 0·5 nA whereas in rat MNTB neurones, the amplitude of the low-threshold current is more than 1 nA at −20 mV. The computational significance of this species difference is not known.

Voltage-gated potassium channels are likely to be composed of a homotetrameric or heterotetrameric complex of subunits from within the *Shaker* superfamily. Auxiliary subunits such as β-subunits can also assemble specifically with these channels and dramatically alter channel kinetics and activation threshold (Rettig *et al.* 1994; Pongs, 1995; Rhodes, Keilbaugh, Barrezueta, Lopez & Trimmer, 1995; Sewing, Roeper & Pongs, 1996; Yu, Xu & Li, 1996). Given the very large number of potassium channel subunits that have been cloned, it has been difficult to correlate expression of particular potassium channel subunits with specific electrophysiological properties of native cells. In part, this is because the kinetic properties of many channel subunits are rather similar and there are few subunit-specific antagonists or toxins (in marked contrast to calcium channels, for instance). A combination of several distinctive biophysical and pharmacological features such as the rapid kinetics, high activation threshold and sensitivity to submillimolar concentration of TEA of the mammalian *Shaw* subfamily channel Kv3.1 differentiates this channel from other cloned channels. Because immunohistochemical evidence suggests that Kv3.3, a slowly inactivating channel, is also expressed in MNTB neurones although less abundantly (Weiser *et al.* 1994), we cannot exclude the possibility that Kv3.1 and Kv3.3 are linked in heteromultimers and account for I_{HT} in MNTB neurones. Nevertheless, our results suggest that the Kv3.1 channel is likely to be the predominant high-threshold potassium channel in the soma. This is supported by two experimental observations. First, the rates of activation of I_{HT} in MNTB neurones closely match those of homomultimeric Kv3.1 channels in CHO cells with a correlation coefficient of 0·998. Second, in contrast to the slow inactivating nature of heteromultimeric Kv3.1 and Kv3.3 channels (Vega-Saenz de Miera *et al.* 1994), I_{HT} does not show significant inactivation. Definitive identification of the role of each of these subunits may come from genetic deletion experiments. For example, a recent study using a mouse in which the Kv3.1 gene has been deleted by homologous recombination found some deficit in the auditory startle response (Ho, Grange & Joho, 1997), although detailed analysis of the binaural auditory pathway has yet to be conducted in these mice.

The molecular identity of I_{LT} is not known. Mammalian *Shaker* and *Shaw* subfamily potassium channels are both present in MNTB neurones (Perney *et al.* 1992; Wang, Kunkel, Martin, Schwartzkroin & Tempel, 1993; Weiser *et al.* 1994) and members of these two subfamilies share some common pharmacological properties. For example, virtually all members from these two subfamilies are very sensitive to submillimolar concentrations of 4-aminopyridine. One of the *Shaker* channels, Kv1.1, like the Kv3.1 channel, is highly sensitive to TEA (IC_{50}, ∼0·3–0·4 mM) (Chandy & Gutman, 1995). However, these two subfamilies differ significantly in certain aspects of biophysical and pharmacological properties. For example, Kv1.1 activates at a much more negative threshold than Kv3.1 (Chandy & Gutman, 1995), and the *Shaker* potassium channels such as Kv1.1, Kv1.2 and Kv1.6 are specifically blocked by DTX with IC_{50} less than 30 nM (Stühmer *et al.* 1988; Grissmer *et al.* 1994; Robertson, Owen, Stow, Butler & Newland, 1996). We have taken advantage of these differences and separated DTX-sensitive I_{LT} and DTX-insensitive I_{HT} in MNTB neurones. Our findings in the mouse, like a previous study in the rat (Brew & Forsythe, 1995), support the view that some *Shaker*-like subunits such as Kv1.1 and Kv1.2 channels are likely to be involved in maintaining the fidelity of transmission from the calyx of Held to the MNTB neurone by limiting postsynaptic action potential firing during the EPSP.

Previous studies have shown that the Kv3.1 channel is expressed at high levels in the auditory pathway, including neurones in the rat aVCN and the MNTB, as well as in fast-spiking inhibitory interneurones of hippocampus and striatum (Perney *et al.* 1992; Lenz *et al.* 1994; Weiser *et al.* 1994, 1995; Du *et al.* 1996). Two lines of evidence suggest that there exists a correlation between the high level of Kv3.1 mRNA and translated protein products at least in rat auditory neurones. Using the amino- or carboxyl-directed antibodies against the Kv3.1 channel, our group and others have shown that there is a specific and strong immunoreactivity in rat auditory neurones including those in the MNTB, and that a high level of Kv3.1 mRNA was also found in these cells (Perney *et al.* 1992; Weiser *et al.* 1994; Perney & Kaczmarek, 1997). Furthermore, the large size of Kv3.1-like I_{HT} we have observed in this study suggests, although it does not definitively prove, that Kv3.1 mRNA has been translated into functional channel proteins. Interestingly, these Kv3.1-containing neurones also abundantly express the calcium binding proteins, calbindin and parvalbumin (Kawaguchi, Katsumaru, Kosaka, Heizmann & Hama, 1987; Vater & Braun, 1994; Weiser *et al.* 1995; Du *et al.* 1996; Lohmann & Friauf, 1996). Such a co-localization may enable these neurones to fire at high rates and yet the large calcium influx associated with high-frequency firing can be rapidly buffered.

In conclusion, we have now validated our previous predictions (Kanemasa *et al.* 1995; Perney & Kaczmarek 1997) that the ability of MNTB neurones to phase lock their firing to high-frequency synaptic inputs depends strongly on their ability to repolarize rapidly following each stimulus. Based on a strong correlation in kinetics, voltage dependence and sensitivity to TEA between I_{HT} and homomultimeric Kv3.1 channels in CHO cells, we suggest that I_{HT} represents a population of potassium channels at least partly comprising Kv3.1 channels, and that this current plays a key role in allowing these neurones to achieve this rapid repolarization during high-frequency firing. The current density of I_{HT} in MNTB is extremely high (> 1 nA pF^{-1}, at +60 mV), providing a large pool of available potassium channels for repolarization. The very rapid activation and deactivation kinetics, and the lack of use-dependent inactivation in Kv3.1 allow these channels to respond rapidly and repeatedly to sustained trains of inputs. More importantly, by using TEA as a tool to dissect out I_{HT} from MNTB neurones, we demonstrated that I_{HT} is essential in maintaining action potential firing at high frequencies (i.e. $>$ 200 Hz). These findings are further borne out by our computer simulations of the effects of elimination of Kv3.1-like currents from cells with the other major conductances of MNTB neurones. Because of the characteristic spherical morphology of the MNTB neurones and of their associated large synaptic endings, a simple, single-compartment model readily mimics the patterns of action potentials that are evoked by repeated stimulation. The modelling suggests that, unlike other potassium currents that activate at more negative potentials, the high voltage threshold for activation of the Kv3.1 channel minimizes the shunting of sodium currents and synaptic currents, and therefore allows a high safety factor for action potential initiation. Collectively, these properties support the notion that the Kv3.1 channel is a key element in the response properties of MNTB.

Barnes-Davies, M. & Forsythe, I. D. (1995). Pre- and postsynaptic glutamate receptors at a giant excitatory synapse in rat auditory brainstem slices. *Journal of Physiology* **488**, 387–406.

Brew, H. M. & Forsythe, I. D. (1995). Two voltage-dependent K^+ conductances with complementary functions in postsynaptic integration at a central auditory synapse. *Journal of Neuroscience* **15**, 8011–8022.

Brownell, W. E. (1975). Organization of the cat trapezoid body and the discharge characteristics of its fibres. *Brain Research* **94**, 413–433.

Chandy, K. G. & Gutman, G. A. (1995). Voltage-gated K^+ channels. In *CRC Handbook of Receptors and Channels*, ed. North, R. A., pp. 1–71. CRC, Boca Raton, FL, USA.

Critz, S. D., Wible, B. A., Lopez, H. S. & Brown, A. M. (1993). Stable expression and regulation of a rat brain K^+ channel. *Journal of Neurochemistry* **60**, 1175–1178.

Du, J., Zhang, L., Weiser, M., Rudy, B. & McBain, C. (1996). Developmental expression and functional characterization of the potassium-channel subunit Kv3.1b in parvalbumin-containing interneurons of the rat hippocampus. *Journal of Neuroscience* **16**, 506–518.

Forsythe, I. D. & Barnes-Davies, M. (1993). The binaural auditory pathway: excitatory amino acid receptors mediate dual time course excitatory postsynaptic currents in the rat medial nucleus of the trapezoid body. *Proceedings of the Royal Society* B **251**, 151–157.

Grissmer, S., Nguywn, A. N., Aiyar, J., Hanson, D. C., Mather, R. J., Gutman, G. A., Karmilowicz, M. J., Auperin, D. D. & Chandy, K. G. (1994). Pharmacological characterization of five cloned voltage-gated K^+ channels, types Kv1.1, 1.2, 1.3, 1.5, and 3.1, stably expressed in mammalian cell lines. *Molecular Pharmacology* **45**, 1227–1234.

Guinan, J. J., Norris, B. E. & Guinan, S. S. (1972). Single auditory units in the superior olivary complex II: locations of unit categories and tonotopic organization. *International Journal of Neuroscience* **4**, 147–166.

Ho, C. S., Grange, R. W. & Joho, R. H. (1997). Pleiotropic effects of a disrupted K^+ channel gene: Reduced body weight, impaired motor skill and muscle contraction, but no seizures. *Proceedings of the National Academy of Sciences of the USA* **94**, 1533–1538.

Isaacson, J. S. & Walmsley, B. (1995). Counting quanta: direct measurements of transmitter release at a central synapse. *Neuron* **15**, 875–884.

Kanemasa, T., Gan, L., Perney, T. M., Wang, L.-Y. & Kaczmarek, L. K. (1995). Electrophysiological and pharmacological characterization of a mammalian Shaw channel expressed in NIH 3T3 fibroblasts. *Journal of Neurophysiology* **74**, 207–217.

Kawaguchi, Y., Katsumaru, H., Kosaka, T., Heizmann, C. W. & Hama, K. (1987). Fast spiking cells in rat hippocampus CA1 region contain the calcium binding protein parvalbumin. *Brain Research* **416**, 469–374.

Konishi, M., Takahashi, T. T., Wagner, H., Sullivan, W. E. & Carr, C. E. (1989). Neurophysiological and anatomical substrates of sound localization in the owl. In *Auditory Function, Neurobiological Bases of Hearing*, ed. Edelman, G. M., Gall, W. E. & Cowan, W. M., pp. 721–746. John Wiley and Sons, New York.

Lenz, S., Perney, T., Qin, Y., Robbins, E. & Chesselet, M. F. (1994). GABA-ergic interneurons of the striatum express the Shaw-like potassium channel Kv3.1. *Synapse* **18**, 55–66.

Lohmann, C. & Friauf, E. (1996). Distribution of the calcium-binding proteins parvalbumin and calretinin in the auditory brainstem of adult and developing rats. *Journal of Comparative Neurology* **367**, 90–109.

Luneau, C. J., Williams, J. B., Marshall, J., Levitan, E. S., Oliva, C. R., Smith, J. S., Antanavage, J., Folander, K., Stein, R. B., Swanson, R., Kaczmarek, L. K. & Buhrow, S. A. (1991). Alternative splicing contributes to K^+ channel diversity in the mammalian central nervous system. *Proceedings of the National Academy of Sciences of the USA* **88**, 3932–3936.

Magistretti, J., Mantegazza, M., Guatteo, E. & Wanke, E. (1996). Action potentials recorded with patch-clamp amplifiers: are they genuine? *Trends in Neurosciences* **19**, 530–534.

Manis, P. B. & Marx, S. O. (1991). Outward currents in isolated ventral cochlear nucleus neurons. *Journal of Neuroscience* **11**, 2865–2880.

Perney, T. M. & Kaczmarek, L. K. (1997). Localization of a high threshold potassium channel in the rat cochlear nucleus. *Journal of Comparative Neurology* **386**, 178–202.

Perney, T. M., Marshall, J., Martin, K. A., Hockfield, S. & Kaczmarek, L. K. (1992). Expression of the mRNAs for the Kv3.1 potassium channel gene in the adult and developing rat brain. *Journal of Neurophysiology* **68**, 756–766.

Pongs, O. (1995). Regulation of the activity of voltage-gated potassium channels by β-subunits. *Journal of Neuroscience* **7**, 137–146.

Raleigh, R. (1907). On our perception of sound direction. *Philosophical Magazine* **13**, 214–232.

Raman, I. M., Zhang, S. & Trussell, L. O. (1994). Pathway-specific variants of AMPA receptors and their contribution to neuronal signaling. *Journal of Neuroscience* **14**, 4998–5010.

Rettig, J., Heinemann, S. H., Wunder, F., Lorra, C., Parcej, D. N., Dolly, J. O. & Pongs, O. (1994). Non-inactivating voltage-gated potassium channels are converted to A-type channels by association with a β-subunit. *Nature* **369**, 289–294.

Reyes, A. D., Rubel, E. W. & Spain, W. J. (1994). Membrane properties underlying the firing of neurons in the avian cochlear nucleus. *Journal of Neuroscience* **14**, 5352–5364.

Rhodes, K., Keilbaugh, S. A., Barrezueta, N. X., Lopez, K. L. & Trimmer, J. S. (1995). Association and colocalisation of K channel α- and β-subunit polypeptide in rat brain. *Journal of Neuroscience* **15**, 5360–5371.

Robertson, B., Owen, D., Stow, J., Butler, C. & Newland, C. (1996). Novel effects of dendrotoxin homologues on subtypes of mammalian Kv1 potassium channels expressed in *Xenopus* oocytes. *FEBS Letters* **383**, 26–30.

Sewing, S., Roeper, J. & Pongs, O. (1996). Kvβ1 subunit binding specific for *Shaker*-related potassium channel α-subunit. *Neuron* **16**, 455–463.

Stühmer, W., Stocker, M., Sakmann, B., Seeburg, P., Baumann, A., Grupe, A. & Pongs, O. (1988). Potassium channels expressed from rat brain cDNA have delayed rectifier properties. *FEBS Letters* **242**, 199–206.

Vater, M. & Braun, K. (1994). Parvalbumin, calbindin D-28k, and calretinin immunoreactivity in the ascending auditory pathway of horseshoe bats. *Journal of Comparative Neurology* **341**, 534–558.

Vega-Saenz de Miera, E., Weiser, M., Kentros, C., Lau, D., Moreno, H., Serodio, P. & Rudy, B. (1994). Shaw-related K^+ channels in mammals. In *Handbook of Membrane Channels*, pp. 41–78. Academic Press, New York.

Wang, H., Kunkel, D. D., Martin, T. M., Schwartzkroin, P. A. & Tempel, B. L. (1993). Heteromultimeric K^+ channels in terminal and juxtaparanodal regions of neurons. *Nature* **365**, 75–79.

Warchol, M. E. & Dallos, P. (1990). Neural coding in the chick cochlear nucleus. *Journal of Comparative Neurology* **A166**, 721–734.

Weiser, M., Bueno, E., Sekirnjak, C., Marton, M. E., Baker, H., Hillman, D., Chen, S., Thornhill, W., Ellisman, M. & Rudy, B. (1995). The potassium channel subunit KV3.1b is localized to somatic and axonal membranes of specific populations of CNS neurons. *Journal of Neuroscience* **15**, 4298–4314.

Weiser, M., Vega-Saenz de Miera, E., Kentros, C., Moreno, H., Franzen, L., Hillman, D., Baker, H. & Rudy, B. (1994). Differential expression of Shaw-related K^+ channels in the rat central nervous system. *Journal of Neuroscience* **14**, 949–972.

Wu, S. H. & Kelly, J. B. (1993). Response of neurons in the lateral superior olive and medial nucleus of the trapezoid body to repetitive stimulation: intracellular and extracellular recordings from mouse brain slice. *Hearing Research* **68**, 189–201.

Yu, W., Xu, J. & Li, M. (1996). NAB domain is essential for the subunit assembly of both α-α and α-β subunit complexes of *Shaker*-like potassium channels. *Neuron* **16**, 441–453.

Zhang, S. & Trussell, L. O. (1994). A characterization of excitatory postsynaptic potentials in the avian nucleus magnocellularis. *Journal of Neurophysiology* **72**, 705–718.

Acknowledgements

We thank Neil Magoski and Benjamin White for comments on the manuscript. This work was supported by an NIH grant (to L.K.K.) and a Wellcome Trust grant (to I.D.F.). L.-Y.W. was sponsored in part by a Human Frontier Science Program Short-Term Fellowship and postdoctoral fellowships from the James Hudson Brown–Alexander B. Coxe Foundation and the Eppley Foundation for Research. I.D.F. is a Wellcome Senior Research Fellow in Basic Biomedical Sciences.

Corresponding author

L. K. Kaczmarek: Department of Pharmacology, Yale University School of Medicine, 333 Cedar Street, New Haven, CT 06520, USA.

Email: Kaczmarek@Yale.edu

Author's present address

L.-Y. Wang: Division of Neurology and The Epilepsy Research Program, Hospital for Sick Children Research Institute, 555 University Avenue, Toronto, Ontario, Canada M5G 1X8.